Supplementary information

Supplementary Figure 1: Evaluation of quantification accuracy using dilution based label-free quantification.

To test the validity of the 1.5-fold cut off chosen in this study for the identification of insulin sensitive interactions, samples derived from chico-affinity purification experiments were diluted into samples from GFP control purifications in a 1:1 (Dilution A) and 1:1.5 (Dilution B) GFP to chico ratio. Three technical replicates were analyzed by LC-MS/MS. (A) Summary of protein quantification using label free quantitative AP-MS. The table lists average intensities of all detected peptides corresponding to the indicated proteins (chico, insulin receptor (InR), 14-3-3 epsilon, 14-3-3 zeta) relative to the median intensity of the ten most intense GFP peptides. Peptide features differing by more than two standard deviations from the average intensity were discarded as outliers before calculation of the intensity ratios (List of all quantified peptide features are shown in Supplementary Table 9). Average intensity ratios between dilutions A and B are shown and correspond well to the values expected from the 1:1.5 dilution. In addition p-values from a Student's t-Test probing the statistical significance of the measured enrichments are shown. As expected, the GFP abundance shows a measured 1:1 ratio (GFP amounts were equal in dilution sample A and B) with p-values indicating no significant difference between the two dilutions A and B. Chico as well as chico interactors on the other hand show an abundance ratio of about 1.5-fold matching the expected fold change with high confidence based on t-test analysis. (B) Bar chart displaying the relative intensities between dilution experiment A and B for indicated proteins from GFP and chico purifications. Error bars represent s.e.m..

Supplementary Figure 2: Sequence alignment of Tel2 orthologs. *Drosophila* lqfR-PD (NP_732736) has been aligned to Tel2 orthologs from *H. sapiens* (NP_057195) and *M. musculus* (NP_082156) using the Indonesia program (see also Takai et al, 2010). The N-terminal extension of lqfR-PD, which does not align, contains the ENTH domain typical for proteins of the epsin family.

Supplementary Figure 3: Co-purification of dTTT components in Kc167 cells. (A-C) *Drosophila* Kc167 cells have been transiently transfected with combinations of the following constructs allowing inducible expression of HA- or GST-tagged fusion proteins: *pMHW-dTOR* (A), *pMHW-CG16908* (B), *pMHW-spag* (C), *pMW-GST-lqfR-RC* (A-C), *pMW-GST-lqfR-RD* (A-C) and *pMW-GST-Spag* (A). Effectene (Qiagen) has been used for transfection according to the manual. Three days following transfection, expression of the fusion proteins has been induced by addition of $CuSO_4$ for 16 h followed by cell lysis, affinity

purification using glutathione sepharose 4B (GE Healthcare; IP of GST-tagged proteins) and Western blotting. The combinations of the expressed fusion proteins are indicated above the lanes. As a negative control, Kc167 cells have been analyzed in the absence of expressed GST-tagged construct. The blots were probed with antibodies as indicated on the left side and the numbers on the right side present molecular weight markers. Unspecific protein bands are marked by asterisks (*). Consistent with our proposed model on the dTTT complex, purified lqfR-PD, (but not the smaller isoform lqfR-PC, see (D)) contains dTOR (A), the product of *CG16908* (B) and Spaghetti (C). In addition, dTOR was also detected in purified Spaghetti complexes (A). (D) Scheme to illustrate the lqfR-PC and lqfR-PD isoforms. Alternative splicing of the precursor mRNA of *lqfR* results in two transcripts (*lqfR-RC* and *lqfR-RD*) and two protein isoforms (lqfR-PC and lqfR-PD), which exhibit different C-terminal extensions. Only the last exon of lqfR-PD, which is not present in lqfR-PC, shows homology to Tel2 orthologs (see also Supplemental Figure 1) explaining the interaction of lqfR-PD, but not of lqfR-PC, with components of the dTTT complex. Exons are indicated by black boxes and white boxes illustrate either the 5'UTR or the different 3'UTRs. Arrows indicate the transcriptional start site.

Supplementary Figure 4: Box plots summarizing the results of RNAi-mediated depletion of network components on the phosphorylation levels of S6K, PKB and 4E-BP. Identified network components were depleted by RNAi in Kc167 cells as indicated below the diagrams (A-C). Total cell extracts were analyzed by immunoblotting and the band intensities obtained with anti-P-4EBP (T37/46; A), anti-P-S6K (S398; B) and anti-P-PKB (S505; C) were quantified (see Materials and Methods). The band intensities observed in total extracts of cells treated with RNAi against EGFP were set to 100%. At least two independent measurements have been performed for each RNAi and the box plots illustrate the data. Each box represents the middle 50% of the data and the line within each box indicates the median, which was used to generate the heat map in Figure 5. The ends of the vertical lines indicate the maximum and minimum data values.

Supplementary Table 1: List of all bait proteins used in this study.

Supplementary Table 2: High confidence interaction data. List of all high confidence protein-protein interactions that passed data filtering. Peptide samples derived from affinity purifications were analyzed

by LC-MS/MS and proteins were identified using the SEQUEST algorithm. Semi-quantitative interaction scoring was carried out using the SAINT 2.0 algorithm (see Materials and Methods). Spectrum counts of bait experiments were grouped based on insulin stimulation (Insulin treatment: 0=untreated, 100=treated) and counts of individual replicate experiments (Exp. A and Exp. B) are listed. In addition, spectrum counts from 24 individual control purifications were summed and divided into 4 groups (Exp. A,B,C,D). Based on SAINT scoring, all accepted protein-protein interactions are listed. In the first step network components were accepted if their SAINT score (AvgP) was at least 0.99. In a second step, for interactions between defined network components a minimum SAINT score of 0.8 was accepted. In addition, remaining cytoskeleton, heat shock and ribosomal proteins were excluded from the high confidence data set (see Supplementary Table 3).

Supplementary Table 3: List of 17 frequent contaminant proteins removed from the data set.

Supplementary Table 4: Peptide and protein prophet scores for the identified network components.

Supplementary Table 5: Comparison of the experimentally obtained *Drosophila* protein-protein interactions to known interaction information. Known interaction information in *Drosophila* was retrieved from DroID version 4.0 (www.droidb.org). Human and yeast orthologues mapping was performed using biomart version 0.7 (www.biomart.org) and known interaction information for yeast was retrieved from the Biogrid (www.thebiogrid.org) version 2.0.53 and DroID. Human orthologous interactions were identified using www.droidb.org and an in-house database including 61263 human PPIs.

Supplementary Table 6: Insulin dependent dynamics of the InR/TOR interaction proteome. Overview on the quantified data set to reveal insulin regulated interactions. All protein interactions passing the SAINT confidence threshold were tested for insulin sensitivity. Peptide samples were analyzed in a three step dilution of insulin treated and untreated samples (0, 30, 100% insulin treated sample) on a LTQ-FT instrument. Label-free quantification was performed on the individual dilution experiments and the peptide intensities were normalized to the individual bait protein intensities. Intensity of aligned peptide features were divided by the most intense feature within the dilution series (see also Material and Methods). Protein profiles were judged as insulin sensitive interactions when passed the following criteria: at least two aligned features in a peptide profile, correlation coefficient of at least 0.5 and individual

enrichment factors showed a minimum change of 1.5 fold. The maximum fold-change was set to 10. The initial list of quantified peptide features are listed in Supplementary Table 7.

Supplementary Table 7: List of peptide intensities derived from of dilution based label-free quantitative experiments used to obtain Insulin dependent dynamics of the InR/TOR interaction proteome.

Supplementary Table 8: Orthologous TTT components found in *D.melanogaster, S.cerevisiae* and *H.sapiens.*

Supplementary Table 9: List of all quantified peptide features used to evaluate the quantification accuracy using dilution based label-free quantification (Supplementary Figure 1). Raw peptide intensities before outlier detection are provided for GFP, chico, InR, 14-3-3epsilon and 14-3-3zeta.

Supplementary Table 10: Quantitative analysis of dTOR complexes using directed MS. List of MS1 signal intensities obtained for dTOR core components. Signal intensities of TOP3 peptides of indicated dTOR core components present in dTOR, dGβL, dRictor and dRaptor purifications were obtained by label-free quantification using Progenesis software. Average MS1 signal intensities of TOP3 peptides of selected dTOR components within individual AP-MS experiments are shown. Experiments are indexed with 1 and 3 or 2 and 4 for experiments performed on either insulin stimulated or unstimulated cells respectively.

Supplementary Table 11: List of all oligo nucleotides used in systematic RNAi experiments.

A

Description	Dilution A			Dilution B			Avg. Intensity ratio	p-value T-test
	GFP/chico (1:1) Exp.1	GFP/chico (1:1) Exp.2	GFP/chico (1:1) Exp.3	GFP/chico (1:1.5) Exp.1	GFP/chico (1:1.5) Exp.2	GFP/chico (1:1.5) Exp.3		
chico	2.67	2.70	2.70	4.01	4.42	3.90	1.58	0.00088
Inr	0.15	0.15	0.15	0.23	0.26	0.24	1.65	0.00056
14-3-3epsilon	0.72	0.73	0.71	1.17	1.19	1.12	1.59	0.00004
14-3-3zeta	1.75	1.75	1.83	2.67	2.88	2.64	1.51	0.00030
Green fluorescent protein	2.51	2.49	2.55	2.44	2.52	2.36	1.01	0.21392

B

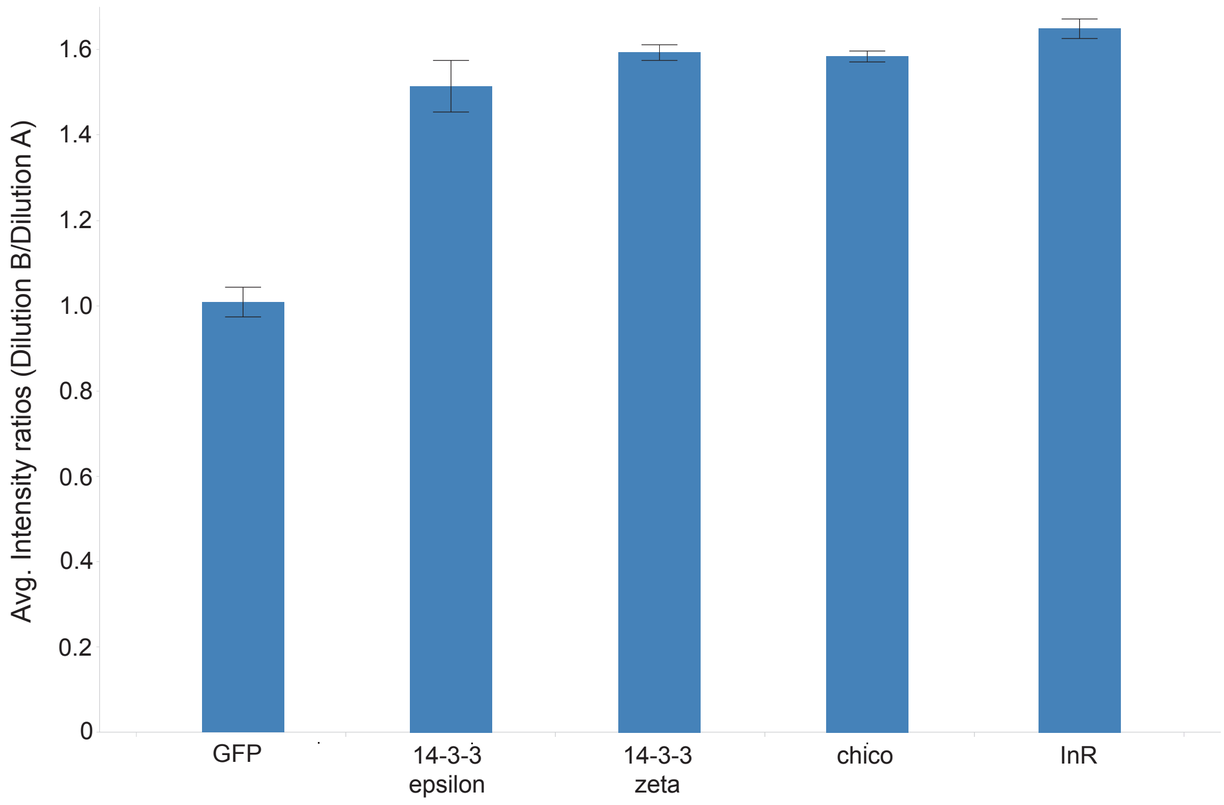

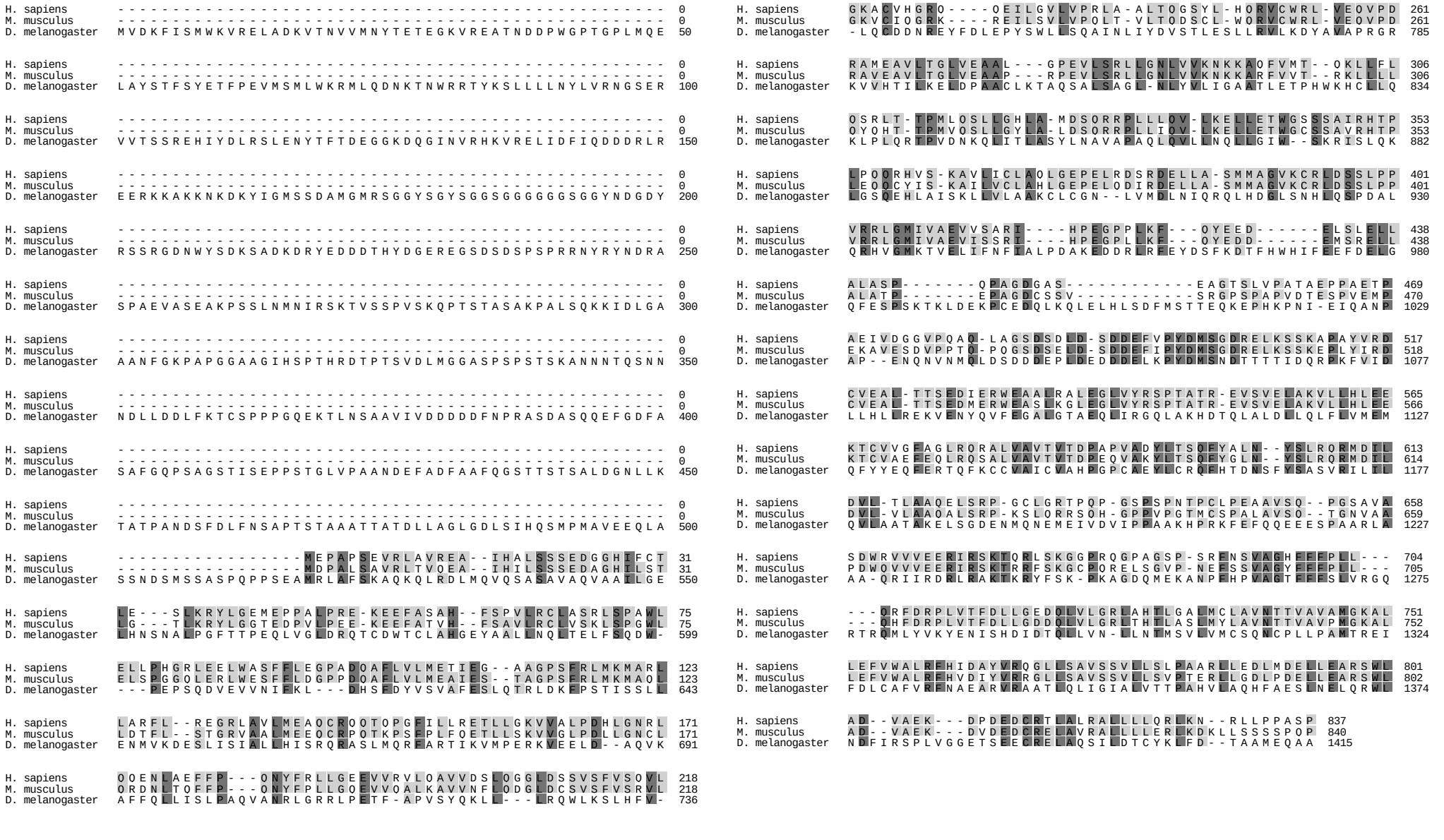
H. sapiens
M. musculus
D. melanogaster

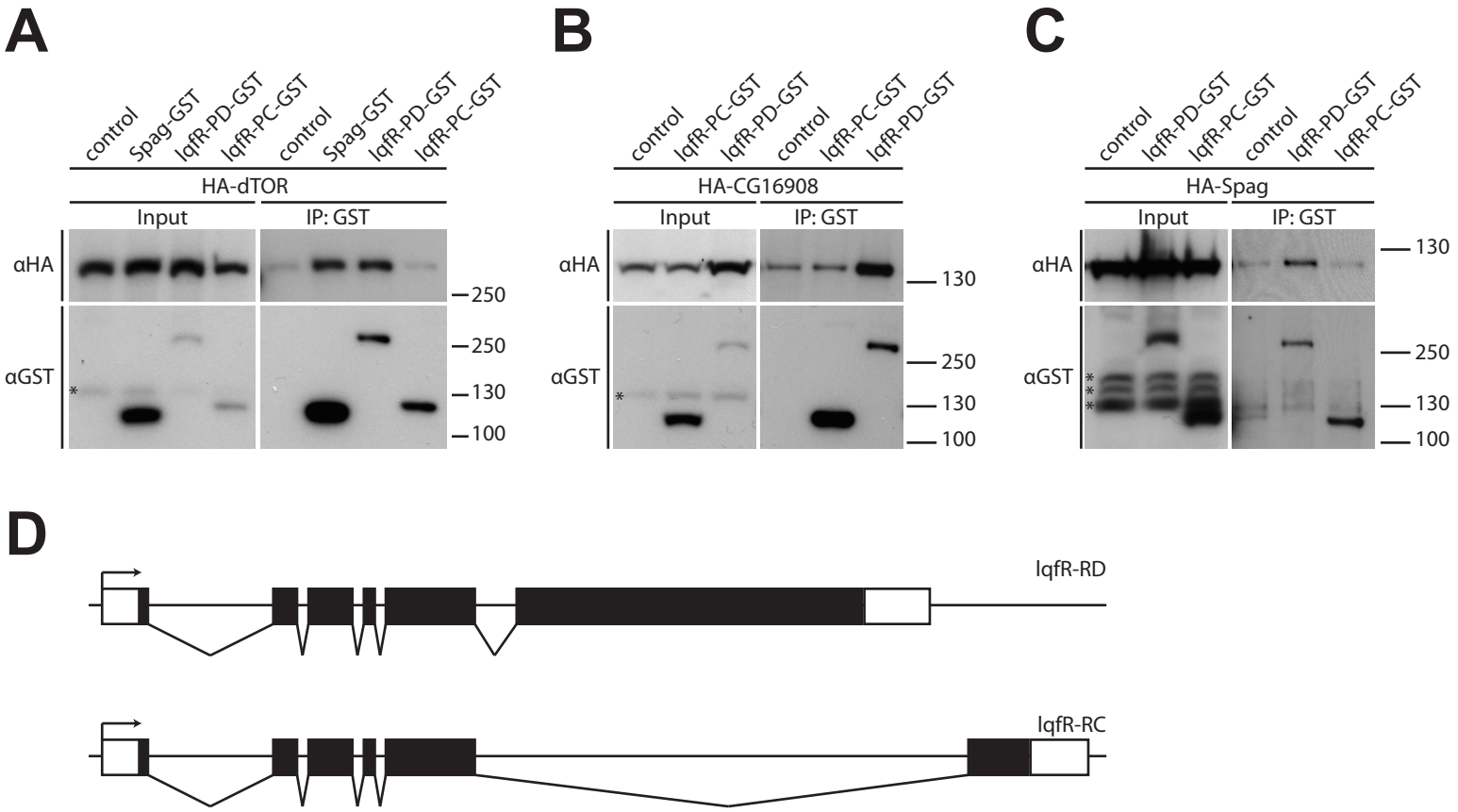
A
control
Spag-GST
lqfR-PD-GST
lqfR-PC-GST
control
Spag-GST
lqfR-PD-GST
lqfR-PC-GST
HA-dTOR
Input
IP: GST
αHA
αGST
250
250
130
100
B
control
lqfR-PC-GST
lqfR-PD-GST
control
lqfR-PC-GST
lqfR-PD-GST
HA-CG16908
Input
IP: GST
αHA
αGST
130
250
130
100
C
control
lqfR-PD-GST
lqfR-PC-GST
control
lqfR-PD-GST
lqfR-PC-GST
HA-Spag
Input
IP: GST
αHA
αGST
130
250
130
100

D
lqfR-RD
lqfR-RC

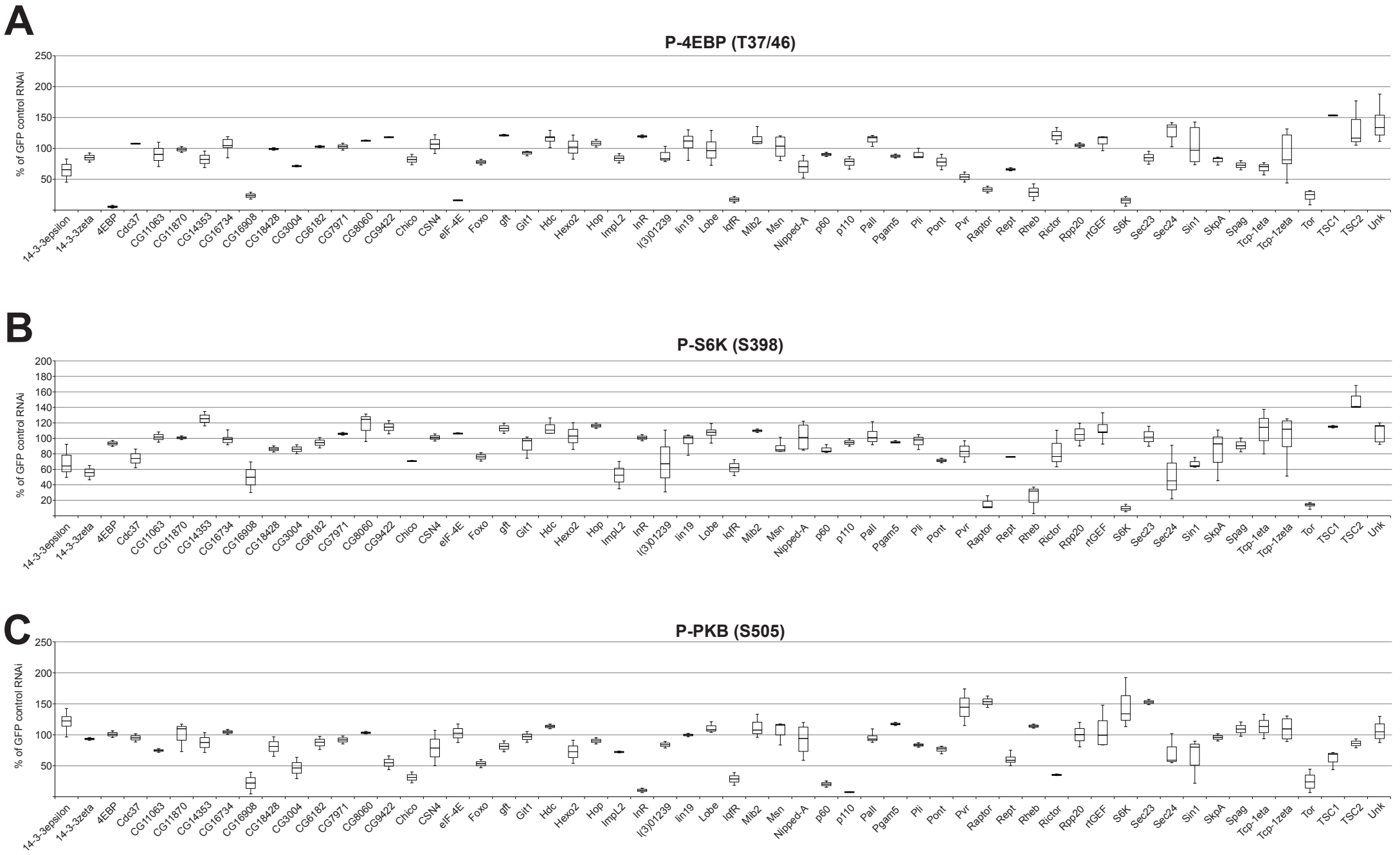
A
P-4EBP (T37/46)
% of GFP control RNAi
250
200
150
100
50
14-3-3epsilon
14-3-3zeta
4EBP
Cdc37
CG11063
CG11870
CG14353
CG16734
CG16908
CG18428
CG3004
CG6182
CG7971
CG8060
CG9422
Chico
CSN4
eIF-4E
Foxo
gft
Git1
Hdc
Hexo2
Hop
ImpL2
InR
l(3)01239
lin19
Lobe
lqfR
Mlb2
Msn
Nipped-A
p60
p110
Pall
Pgam5
Pli
Pont
Pvr
Raptor
Rept
Rheb
Rictor
Rpp20
rtGEF
S6K
Sec23
Sec24
Sin1
SkpA
Spag
Tcp-1eta
Tcp-1zeta
Tor
TSC1
TSC2
Unk
B
P-S6K (S398)
% of GFP control RNAi
200
180
160
140
120
100
80
60
40
20
C
P-PKB (S505)
% of GFP control RNAi
250
200
150
100
50